WAVELET METHODS FOR SOLVING INTEGRAL AND DIFFERENTIAL EQUATIONS

Many of the phenomena studied in electrical engineering and physics can be described mathematically by second-order partial differential equations (PDEs). Some examples of PDEs are the Laplace, Poisson, Helmholtz, and Schrödinger equations. Each of these equations may be solved analytically in some cases, but not for all cases of interest. These PDEs can often be converted to integral equations. One of the attractive features of integral equations is that boundary conditions are built in and, therefore, do not have to be applied externally (1). Mathematical questions of existence and uniqueness of a solution may be handled with greater ease with the integral form.

Either approach, differential or integral equations, used to represent a physical phenomenon can be viewed in terms of an operator operating on an unknown function in order to produce a known function. In this article we will deal with the linear operator. The linear operator equation is converted to a system of linear equations with the help of a complete set of basis functions which are then solved for the unknown coefficients. The finite-element and finite-difference techniques used to solve PDEs result in sparse and banded matrices, whereas integral equations almost always lead to a dense matrix; an exception is the case when the basis functions, chosen to represent the unknown functions, happen to be the eigenfunctions of the operator.

With the advent of wavelets in the 1980s (although they were known in one form or the other since the beginning of this century), numerical analysts have been presented with a new class of "local" basis functions at their disposal which can significantly improve existing methods. Two of the main properties of wavelets vis-à-vis boundary value problems are their hierarchical nature and the vanishing moments properties. Because of their hierarchical (multiresolution) nature, wavelets at different resolutions are interrelated, a property that makes them suitable candidates for multigrid-type methods in solving PDEs. On the other hand, the vanishing moment property by virtue of which wavelets, when integrated against a function of certain order, make the integral zero, is attractive in sparsifying a dense matrix generated by an integral equation.

In the next section, we provide some definitions and properties of wavelets that are relevant to understanding the materials presented in this article. A complete exposition of the application of wavelets to integral and differential equation is beyond the scope of this article. Our objective is to provide the reader with some preliminary theory and results on the application of wavelets to boundary value problems and give references where more details may be found. Since we most often encounter integral equations in electrical engineering problems, we will emphasize their solutions using wavelets. We give a few examples of commonly occurring integral equations. The first and the most important step in solving integral equations is to transform them into a set of linear equations. Both conventional and wavelet-based methods in generating matrix equations are discussed. Some numerical results are presented which illustrate the advantages of the wavelet-based technique. We also discuss wavelets on the bounded interval. Some of the techniques applied to solving integral equations are useful for differential equations as well. At the end of this article we briefly describe the applications of wavelets in PDEs and provide references where readers can find further information.

WAVELET PRELIMINARIES

In this section we briefly describe the basics of wavelet theory to facilitate further discussion in this article. More details on multiresolution and other properties of wavelets may be found elsewhere in this encyclopedia. Readers may also refer to Refs. 2–10.

As pointed out before, multiresolution analysis (MRA) plays an important role in the application of wavelets to boundary value problems. In order to achieve MRA, we must have a finite-energy function (square integrable on the real line) $\phi(x) \in L^2(\mathbb{R})$, called a scaling function, that generates a nested sequence of subspaces

$$\{0\} \leftarrow \cdots \subset V_{-1} \subset V_0 \subset V_1 \subset \cdots \rightarrow L^2 \tag{1}$$

and satisfies the dilation (refinement) equation, namely,

$$\phi(x) = \sum_k p_k \phi(2x - k) \tag{2}$$

with $\{p_k\}$ belonging to the set of square summable bi-infinite sequences. The number 2 in Eq. (2) signifies "octave levels." In fact this number could be any rational number, but we will discuss only octave levels or scales. From Eq. (2) we see that the function $\phi(x)$ is obtained as a linear combination of a scaled and translated version of itself, and hence the name scaling function.

The subspaces V_j are generated by $\phi_{j,k}(x) := 2^{j/2}\phi(2^j x - k)$, $j, k \in \mathbb{Z}$, where $\mathbb{Z} := \{. . ., -1, 0, 1, . . .\}$. For each scale j, since $V_j \subset V_{j+1}$, there exists a complementary subspace W_j of V_j in V_{j+1}. This subspace W_j is called "wavelet subspace" and is generated by $\psi_{j,k}(x) := 2^{j/2}\psi(2^j x - k)$, where $\psi \in L^2$ is called the "wavelet." From the above discussion, these results follow easily:

$$\begin{cases} V_{j_1} \cap V_{j_2} = V_{j_1}, & j_1 > j_2 \\ W_{j_1} \cap W_{j_2} = \{0\}, & j_1 \neq j_2 \\ V_{j_1} \cap W_{j_2} = \{0\}, & j_1 \leq j_2 \end{cases} \tag{3}$$

The scaling function ϕ exhibits low-pass filter characteristics in the sense that $\hat{\phi}(0) = 1$, where a hat over the function denotes its Fourier transform. On the other hand, the wavelet function ψ exhibits bandpass filter characteristic in the sense that $\hat{\psi}(0) = 0$. Some of the important properties that we will use in this article are given below:

- *Vanishing Moment.* A wavelet is said to have a vanishing moment of order m if

$$\int_{-\infty}^{\infty} x^p \psi(x)\, dx = 0, \qquad p = 0, \ldots, m - 1 \tag{4}$$

All wavelets must satisfy the above condition for $p = 0$.

J. Webster (ed.), *Wiley Encyclopedia of Electrical and Electronics Engineering*. Copyright © 1999 John Wiley & Sons, Inc.

- *Orthonormality*. The wavelets $\{\psi_{j,k}\}$ form an orthonomal (o.n.) basis if

$$\langle \psi_{j,k}, \psi_{l,m} \rangle = \delta_{j,l}\delta_{k,m} \qquad \text{for all } j,k,l,m \in \mathbb{Z} \tag{5}$$

where $\delta_{p,q}$ is the Kronecker δ defined in the usual way as

$$\delta_{p,q} = \begin{cases} 1, & p = q; \\ 0, & \text{otherwise} \end{cases} \tag{6}$$

The inner product $\langle f_1, f_2 \rangle$ of two square integrable functions f_1 and f_2 is defined as

$$\langle f_1, f_2 \rangle := \int_{-\infty}^{\infty} f_1(x) f_2^*(x)\, dx$$

with $f_2^*(x)$ representing the complex conjugation of f_2.

- *Semiorthogonality*. The wavelets $\{\psi_{j,k}\}$ form a semiorthogonal (s.o.) basis if

$$\langle \psi_{j,k}, \psi_{l,m} \rangle = 0;\ j \neq l \qquad \text{for all } j,k,l,m \in \mathbb{Z} \tag{7}$$

Given a function $f(x) \in L^2$, the decomposition into various scales begins by mapping the function into a sufficiently high-resolution subspace V_M, that is,

$$L^2 \ni f(x) \mapsto f_M = \sum_k a_{M,k}\phi(2^M t - k) \in V_M \tag{8}$$

Now since

$$\begin{aligned} V_M &= W_{M-1} + V_{M-1} \\ &= W_{M-1} + W_{M-2} + V_{M-2} \\ &= \sum_{n=1}^{N} W_{M-n} + V_{M-N} \end{aligned} \tag{9}$$

we can write

$$f_M(x) = \sum_{n=1}^{N} g_{M-n}(x) + f_{M-N}(x) \tag{10}$$

where $f_{M-N}(x)$ is the coarsest approximation of $f_M(t)$ and

$$f_j(x) = \sum_k a_{j,k}\phi(2^j t - k) \in V_j \tag{11}$$

$$g_j(x) = \sum_k w_{j,k}\psi(2^j t - k) \in W_j \tag{12}$$

If the scaling functions and wavelets are orthonormal, it is easy to obtain the coefficients $\{a_{j,k}\}$ and $\{w_{j,k}\}$. However, for the s.o. case, we need a dual scaling function ($\tilde{\phi}$) and dual wavelet ($\tilde{\psi}$). Dual wavelets satisfy the "biorthogonality condition," namely,

$$\langle \psi_{j,k}, \tilde{\psi}_{l,m} \rangle = \delta_{j,l} \cdot \delta_{k,m},\ j,k,l,m \in \mathbb{Z} \tag{13}$$

For the s.o. case, both ψ and $\tilde{\psi}$ belong to the same space W_j for an appropriate j; likewise ϕ and $\tilde{\phi}$ belong to V_j. One of the difficulties with s.o. wavelets is that their duals do not have compact support. We can achieve compact support for both $\tilde{\phi}$ and $\tilde{\psi}$ if we forgo the orthogonality requirement that $V_j \perp W_j$. In such a case we get "biorthogonal wavelets" (11) and two MRAs, $\{V_j\}$ and $\{\tilde{V}_j\}$. In this article we will discuss application of o.n. and s.o. wavelets only.

INTEGRAL EQUATIONS

Integral equations appear frequently in practice, particularly the first-kind integral equations (12) in inverse problems. These equations can be represented as

$$L_K f = \int_a^b f(x')K(x,x')\, dx' = g(x) \tag{14}$$

where $f(x)$ is an unknown function, $K(x, x')$ is the known kernel which might be the system impulse response or Green's function, and $g(x)$ is the known response functions.

For instance, the electric surface current J_{sz} on an infinitely long metallic cylinder illuminated by an electromagnetic plane wave that is transverse magnetic (TM) to the z direction, as shown in Fig. 1, is related to the incident electric field via an integral equation

$$j\omega\mu_0 \int_C J_{sz}(l')G(l,l')\, dl' = E_z^i(l) \tag{15}$$

where

$$G(l,l') = \frac{1}{4j} H_0^{(2)}(k_0|\boldsymbol{\rho}(l) - \boldsymbol{\rho}(l')|) \tag{16}$$

with the wavenumber, $k_0 = 2\pi/\lambda_0$. The electric field, E_z^i, is the z component of the incident electric field and $H_0^{(2)}$ is the second-kind Hankel function of order 0, and λ_0 is the wavelength in free space. Here, the contour of integration has been parameterized with respect to the chord length. The field component E_z^i can be expressed as

$$E_z^i(l) = E_0 \exp[jk_0(x(l)\cos\phi_i + y(l)\sin\phi_i)] \tag{17}$$

where ϕ_i is the angle of incidence.

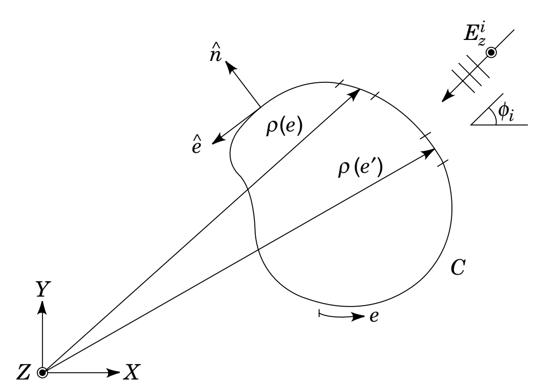

Figure 1. Cross section of an infinitely long metallic cylinder illuminated by a TM plane wave.

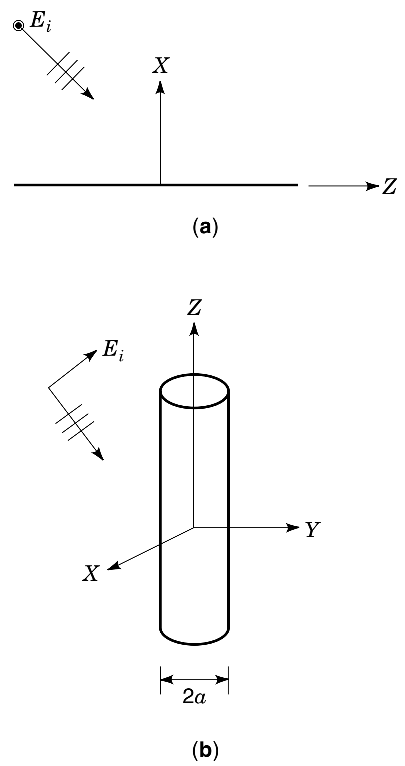

Figure 2. (a) A thin half-wavelength long metallic strip illuminated by a TM wave. (b) A thin wire of length $\lambda/2$ and thickness $\lambda/1000$ illuminated by a plane wave.

Scattering from a thin perfectly conducting strip, as shown in Fig. 2(a), gives rise to an equation similar to Eq. (15). For this case, we have

$$\int_{-h}^{n} J_{sy}(z')G(z,z')\,dz' = E_y^i(z) \tag{18}$$

where $G(z, z')$ is given by Eq. (16).

As a final example of the scattering problem, consider scattering from a thin wire as shown in Fig. 2(b). Here the current on the wire and the incident field are related to each other as

$$\int_{-l}^{l} I(z')K_{\mathrm{w}}(z,z')\,dz' = -E^i(z) \tag{19}$$

where the kernel K_{w} is given by

$$K_{\mathrm{w}}(z,z') = \frac{1}{4\pi j\omega\epsilon_0}\frac{\exp(-jk_0R)}{R^5} \times [(1+jk_0R)\times(2R^2-3a^2)+k_0^2a^2R^2] \tag{20}$$

$$E^i(z) = E_0\sin\theta\exp(jk_0z\cos\theta) \tag{21}$$

This kernel is obtained by interchanging integration and differentiation in the integrodifferential form of Pocklington's equation and by using the reduced kernel distance $R = [a^2 + (z - z')^2]^{1/2}$, where a is the radius of the wire (13).

All of the equations described thus far have the form of a first-kind integral equation, namely,

$$\int_a^b f(x')K(x,x')\,dx' = g(x) \tag{22}$$

where f is the unknown function and the kernel K and the function g are known. Here the objective is to reconstruct the function f from a set of known data (possibly measured) g. The kernel K may be thought of as the impulse response function of the system.

Although we discuss the solution technique for first-kind integral equations only, the method can be easily extended to second-kind equations (14,15) and higher-dimensional integral equations (16).

MATRIX EQUATION GENERATION

As mentioned in the previous section, the first step in solving any integral or differential equation is to convert these into a matrix equation which is then solved for the unknown coefficients which are subsequently used to construct the unknown function.

The goal is to transform Eq. (14) to a matrix equation:

$$Zi = v \tag{23}$$

where Z is a two-dimensional matrix, sometimes referred to as impedance matrix, i is the column vector of unknown coefficients, and v is another column vector related to g. Computation time depends largely upon the way we obtain and solve Eq. (23). In the following section we describe conventional and wavelet basis functions that are used to represent the unknown function.

Conventional Basis Functions

The unknown function $f(x)$ can be written as

$$f(x) = \sum_n i_n b_n(x) \tag{24}$$

where $\{b_n\}$ form a complete set of basis functions. These bases may be "global" (entire domain), extending the entire length $[a, b]$, or they may be "local" (subdomain), covering only a small segment of the interval, or a combination of both. Some of the commonly used subdomain basis functions are shown in Fig. 3.

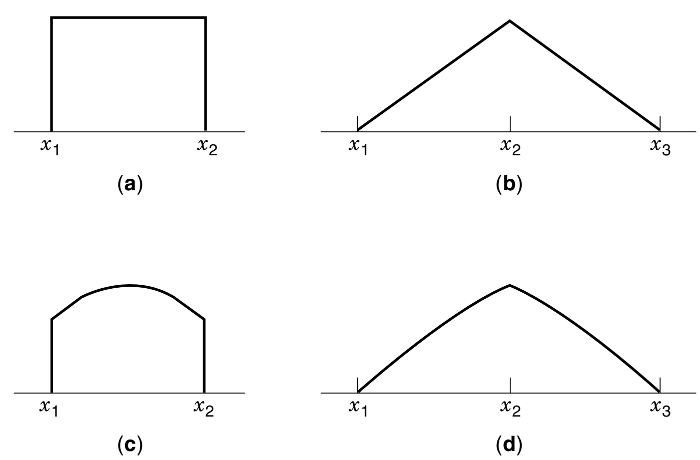

Figure 3. Typical subdomain basis functions: (a) piecewise constant, (b) piecewise linear, (c) piecewise cosine, and (d) piecewise sine functions.

For an exact representation of $f(x)$ we may need an infinite number of terms in the above series. However, in practice, a finite number of terms suffices for a given acceptable error. Substituting the series representation of $f(x)$ into the original Eq. (14), we get

$$\sum_{n=1}^{N} i_n L_K b_n \approx g \tag{25}$$

For the present discussion we will assume N to be large enough so that the above representation is exact. Now by taking the inner product of Eq. (25) with a set of *weighting functions* or *testing functions* $\{t_m: m = 1, . . ., M\}$ we obtain a set of linear equations

$$\sum_{n=1}^{N} i_n \langle t_m, L_K b_n\rangle = \langle t_m, g\rangle, \qquad m = 1, \ldots, M \tag{26}$$

which can be written in the matrix form as

$$[Z_{mn}][i_n] = [v_m] \tag{27}$$

where

$$Z_{mn} = \langle t_m, L_K b_n\rangle, \qquad m = 1, \ldots, M, \quad n = 1, \ldots, N$$
$$v_m = \langle t_m, g\rangle, \qquad m = 1, \ldots, M$$

The solution of the matrix equation gives the coefficients $\{i_n\}$ and thereby the solution of the integral equations. Two main choices of the testing functions are (1) $t_m(x) = \delta(x - x_m)$, where x_m is a discretization point in the domain, and (2) $t_m(x) = b_m(x)$. In the former case the method is called *point matching,* whereas the latter method is known as *Galerkin method.* The method so described and those to be discussed in the following sections are generally referred to as "method of moments" (MoM) (17). We will refer to MoM with conventional bases as "conventional MoM" while the method with wavelet bases will be called "wavelet MoM." Observe that the operator L_K in the preceding paragraphs could be any linear operator—differential as well as integral.

Wavelet Bases

Conventional bases (local or global), when applied directly to the integral equations, generally lead to a dense (fully populated) matrix Z. As a result, the inversion and the final solution of such a system of linear equations are very time-consuming. In later sections it will be clear why conventional bases give a dense matrix while wavelet bases produce sparse matrices. Observe that conventional MoM is a single-level approximation of the unknown function in the sense that the domain of the function ($[a, b]$, for instance) is discretized only once, even if we use nonuniform discretization of the domain. Wavelet MoM, on the other hand, is inherently multilevel in nature, as we will discuss later.

Beylkin et al. (18) first proposed the use of wavelets in sparsifying an integral equation. Alpert et al. (14) used "wavelet-like" basis functions to solve second-kind integral equations. In electrical engineering, wavelets have been used to solve integral equations arising from electromagnetic scattering and transmission line problems (16,19–33). In what follows we briefly describe four different ways in which wavelets have been used in solving integral equations.

Use of Fast Wavelet Algorithm. In this method, the impedance matrix Z is obtained via the conventional method of moments using basis functions such as triangular functions, and then wavelets are used to transform this matrix into a sparse matrix (19,20). Consider a matrix W formed by wavelets. This matrix comprises the decomposition and reconstruction sequences and their translates. We have not discussed these sequences here, but readers may find these sequences in any standard book on wavelets (2–10), for example.

The transformation of the original MoM impedance matrix into the new wavelet basis is obtained as

$$WZW^{\mathrm{T}} \cdot (W^{\mathrm{T}})^{-1} i = Wv \tag{28}$$

which can be written as

$$Z_{\mathrm{w}} \cdot i_{\mathrm{w}} = v_{\mathrm{w}} \tag{29}$$

where W^{T} represents the transpose of the matrix W. The new set of wavelet transformed linear equations are

$$Z_{\mathrm{w}} = WZW^{\mathrm{T}} \tag{30}$$

$$i_{\mathrm{w}} = (W^{\mathrm{T}})^{-1} i \tag{31}$$

$$v_{\mathrm{w}} = Wv \tag{32}$$

The solution vector i is then given by

$$i = W^{\mathrm{T}}(WZW^{\mathrm{T}})^{-1} Wv \tag{33}$$

For orthonormal wavelets $W^{\mathrm{T}} = W^{-1}$ and the transformation (28) is "unitary similar." It has been shown in Refs. 19 and 20 that the impedance matrix Z_{w} is sparse, which reduces the inversion time significantly. Discrete wavelet transform (DWT) algorithms can be used to obtain Z_{w}. Readers may find the details of discrete wavelet transform (octave scale transform) elsewhere in this encyclopedia or in any standard book on wavelets. Sometimes it becomes necessary to compute the wavelet transform at nonoctave scales. Readers are referred to Refs. 34–36 for details of such algorithm.

Direct Application of Wavelets. In another method of applying wavelets to integral equations, wavelets are directly applied; that is, first the unknown function is represented as a superposition of wavelets at several levels (scales) along with the scaling function at the lowest level, prior to using Galerkin's method described before.

In terms of wavelets and scaling functions we can write the unknown function f in Eq. (14) as

$$f(x) = \sum_{j=j_0}^{j_u} \sum_{k=K_1}^{K(j)} w_{j,k} \psi_{j,k}(x) + \sum_{k=K_1}^{K(j_0)} a_{j_0,k} \phi_{j_0,k}(x) \tag{34}$$

where we have used the multiscale property, Eq. (10).

It should be pointed out here that the wavelets $\{\psi_{j,k}\}$ by themselves form a complete set; therefore, the unknown function could be expanded entirely in terms of the wavelets. However, to retain only a finite number of terms in the expansion, the scaling function part of Eq. (34) must be included. In other words, $\{\psi_{j,k}\}$, because of their bandpass filter characteristics, extract successively lower and lower frequency components of the unknown function with decreasing values of the scale parameter j, while $\phi_{j_0,k}$, because of its lowpass filter characteristics, retains the lowest frequency components or the coarsest approximation of the original function.

In Eq. (34), the choice of j_0 is restricted by the order of the wavelet, while the choice of j_u is governed by the physics of the problem. In applications involving electromagnetic scattering, as a "rule of thumb" the highest scale, j_u, should be chosen such that $1/2^{j_u+1}$ does not exceed $0.1\lambda_0$, with λ_0 being the operative wavelength.

When Eq. (34) is substituted in Eq. (14), and the resultant equation is tested with the same set of expansion functions, we get a set of linear equations

$$\begin{bmatrix} [Z_{\phi,\phi}] & [Z_{\phi,\psi}] \\ [Z_{\psi,\phi}] & [Z_{\psi,\psi}] \end{bmatrix} \begin{bmatrix} [a_{j_0,k}]_k \\ [w_{j,n}]_{j,n} \end{bmatrix} = \begin{bmatrix} \langle v, \phi_{j_0,k'} \rangle_{k'} \\ \langle v, \psi_{j',k'} \rangle_{j',k'} \end{bmatrix} \tag{35}$$

where the ψ term of the expansion function and the ϕ term of the testing function give rise to the $[Z_{\phi,\psi}]$ portion of the matrix Z. Similar interpretation holds for $[Z_{\phi,\phi}]$, $[Z_{\psi,\phi}]$, and $[Z_{\psi,\psi}]$.

By carefully observing the nature of the submatrices, we can explain the "denseness" of the conventional MoM and the "sparseness" of the wavelet MoM. Unlike wavelets, the scaling functions discussed in this article do not possess the vanishing moments properties. Consequently, for two pulse or triangular functions ϕ_1 and ϕ_2 (usual bases for the conventional MoM and suitable candidates for the scaling functions), even though $\langle \phi_1, \phi_2 \rangle = 0$ for nonoverlapping support, $\langle \phi_1, L_K\phi_2 \rangle$ is not very small since $L_k\phi_2\rangle$ is not small. On the other hand, as is clear from the vanishing moment property [Eq. (4)] of a wavelet of order m, the integral vanishes if the function against which the wavelet is being integrated behaves as a polynomial of a certain order "locally." Away from the singular points the kernel has a polynomial behavior locally. Consequently, integrals such as $(L_K\psi_{j,n})$ and the inner products involving wavelets are very small for nonoverlapping support.

Because of its "total positivity" property (5, pp. 207–209), the scaling function has a "smoothing" or "variation diminishing" effect on a function against which it is integrated. The smoothing effect can be understood as follows. If we convolve two pulse functions, both of which are discontinuous but totally positive, the resultant function is a linear B-spline (triangular function) which is continuous. Likewise, if we convolve two linear B-splines, we get a cubic B-spline which is twice continuously differentiable. Analogous to these, the function $L_K\phi_{j_0,k}$ is smoother than the kernel K itself. Furthermore, because of the MRA properties that give

$$\langle \phi_{j,k}, \psi_{j',l} \rangle = 0, \qquad j \leq j' \tag{36}$$

the integrals $\langle \phi_{j_0,k'}, (L_K\psi_{j,n}) \rangle$ and $\langle \psi_{j',n'}, (L_K\phi_{j_0,k}) \rangle$ are quite small.

The $[Z_{\phi,\phi}]$ portion of the matrix, although diagonally dominant, usually does not have entries which are very small compared to the diagonal entries. In the conventional MoM case, all the elements of the matrix are of the form $\langle \phi_{j,k'}, (L_K\phi_{j,k}) \rangle$. Consequently, we cannot threshold such a matrix in order to sparsify it. In the wavelet MoM case, the entries of $[Z_{\phi,\phi}]$ occupy a very small portion (5×5 for linear and 11×11 for cubic spline cases) of the matrix, while the rest contain entries whose magnitudes are very small compared to the largest entry; hence a significant number of entries can be set to zero without affecting the solution appreciably.

Wavelets in Spectral Domain. In the previous section, we have used wavelets in the space domain. The local support and vanishing moment properties of wavelet bases were used to obtain a sparse matrix representation of an integral equation. In some applications, particularly in spectral domain methods in electromagnetics, wavelets in the spectral domain may be quite useful. Whenever we have a problem in which the unknown function is expanded in terms of the basis function in the space (time) domain while the numerical computation takes place in the spectral (frequency) domain, we should look at the space-spectral window product in order to determine the efficiency of using a particular basis function. According to the "uncertainty principle," the space-spectral window product of a square integrable function cannot be less than 0.5; the lowest value is possible only for functions of Gaussian class. Because of the nearly optimal space-spectral window product of the cubic spline and the corresponding semiorthogonal wavelet, the improper integrals appearing in many spectral domain formulations of integral equations can be evaluated efficiently. This is due to the fact that higher-order wavelets generally have faster decay in the spectral domain. The spectral domain wavelets have been used to solve the transmission line discontinuity problem in Ref. 16.

Wavelet Packets. The discrete wavelet packet (DWP) similarity transformations have been used to obtain a higher degree of sparsification of the matrix than is achievable using the standard wavelets (31). It has also been shown that the DWP method gives faster matrix–vector multiplication than some of the fast multipole methods.

In the standard wavelet decomposition process, first we map the given function to a sufficiently high resolution subspace (V_M) and obtain the approximation coefficients $\{a_{M,k}\}$ (see section entitled "Wavelet Preliminaries"). The approximation coefficients $\{a_{M-1,k}\}$ and wavelet coefficients $\{w_{M-1,k}\}$ are computed from $\{a_{M,k}\}$. This process continues; that is, the coefficients for the next lower level $M - 2$ are obtained from $\{a_{M-1,k}\}$, and so on. Observe that in this scheme, only approximation coefficients $\{a_{j,k}\}$ are processed at any scale j; the wavelet coefficients are merely the outputs and remain untouched. In a wavelet packet, the wavelet coefficients are also processed which, heuristically, should result in higher degree of sparsity since in this scheme the frequency bands are further divided compared with the standard decomposition scheme.

INTERVALLIC WAVELETS

Wavelets on the real line have been used to solve integral equations arising from electromagnetic scattering and waveguiding problems. The difficulty with using wavelets on the entire real line is that the boundary conditions need to be enforced explicitly. Some of the scaling functions and wavelets must be placed outside the domain of integration. Furthermore, because of truncation at the boundary, the vanishing moment property is not satisfied near the boundary. Also, in signal processing, uses of these wavelets lead to undesirable jumps near the boundaries. We can avoid this difficulty by periodizing the scaling function as (4, Sec. 9.3)

$$\phi^{p}_{j,k} := \sum_{l} \phi_{j,k}(x+l) \tag{37}$$

where the superscript p implies periodic case. Periodic wavelets are obtained in a similar way. It is easy to show that if $\hat{\phi}(2\pi k) = \delta_{k,0}$, which is generally true for the scaling functions, then $\sum_k \phi(x-k) \equiv 1$. If we apply the last relation (which is also known as the "partition of unity") to Eq. (37), we can show that $\{\phi^{p}_{0,0}\} \cup \{\psi^{p}_{j,k};\, j \in \mathbb{Z}^{+} := \{0, 1, 2, \ldots\},\, k = 0, \ldots, 2^{j} - 1\}$ generates $L^2([0, 1])$.

Periodic wavelets have been used by Refs. 28–30. However, as mentioned in Ref. 4, Sec. 10.7, unless the function which is being approximated by the periodized scaling functions and wavelets has the same values at the boundaries, we still have "edge" problems at the boundaries. To circumvent these difficulties, wavelets, constructed especially for a bounded interval, has been introduced in Ref. 33. Details on intervallic wavelets may be found in Refs. 33 and 37–39. Most of the time, we are interested in knowing the formulas for these wavelets rather than delving into the mathematical rigor of their construction. These formulas may be found in Refs. 10 and 33.

Wavelets on a bounded interval satisfy all the properties of regular wavelets that are defined on an entire real line; the only difference is that in the former case, there are a few special wavelets near the boundaries. Wavelets and scaling functions whose support lies completely inside the interval have properties that are exactly the same as those of regular wavelets. As an example, consider semiorthogonal wavelets of order m. For this case the scaling functions (B-splines of order m) have support $[0, m]$, whereas the corresponding wavelet extends the interval $[0, 2m-1]$. If we normalize the domain of the unknown function from $[a, b]$ to $[0, 1]$, then there will be 2^{j} segments at any scale j (discretization step $= 2^{-j}$). Consequently, in order to have at least one complete inner wavelet, the following condition must be satisfied:

$$2^{j} \geq 2m - 1 \tag{38}$$

For j satisfying the above condition, there are $m-1$ boundary scaling functions and wavelets at 0 and 1, and $2^{j} - m + 1$ inner scaling functions and $2^{j} - 2m + 2$ inner wavelets. Figure 4 shows all the scaling functions and wavelets for $m = 2$ at the scale $j = 2$. All the scaling functions for $m = 4$ and $j = 3$ are shown in Fig. 5(a), while Fig. 5(b) gives only the corresponding boundary wavelets near $x = 0$ and one inner wavelet. The rest of the inner wavelets can be obtained by simply translating the first one, whereas the boundary wavelets near $x = 1$ are the mirror images of ones near $x = 0$.

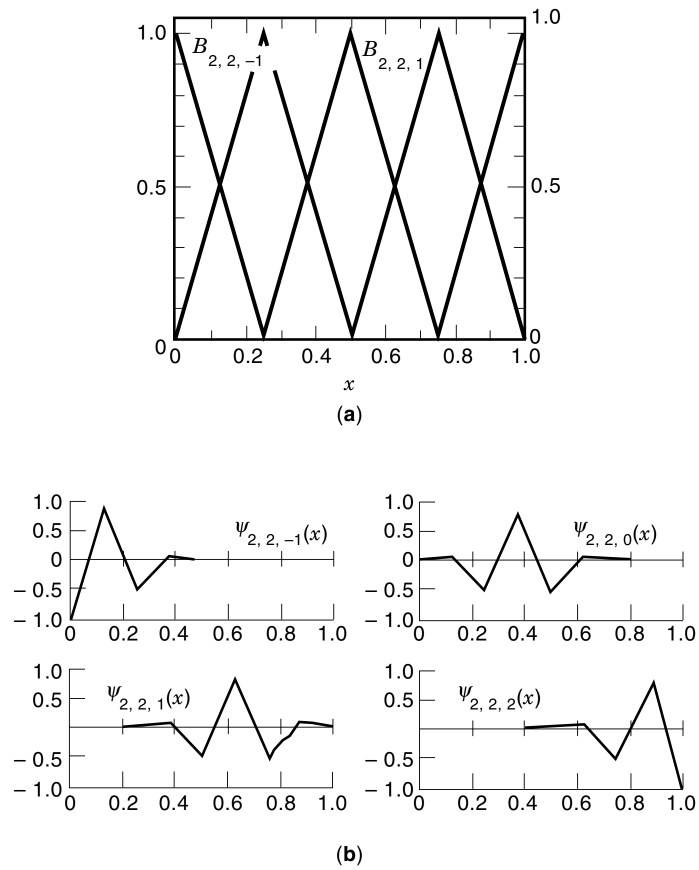

Figure 4. (a) Linear spline ($m = 2$) scaling functions on [0, 1]. (b) Linear spline wavelets on [0, 1]. The subscripts indicate the order of spline (m), scale (j), and position (k), respectively (33).

NUMERICAL RESULTS

In this section we present some numerical examples for the scattering problems described previously. Numerical results for strip and wire problems can be found in Ref. 24. Results for spectral domain applications of wavelets to transmission line discontinuity problems may be found in Ref. 16. For more applications of wavelets to electromagnetic problems, readers may refer to Ref. 32.

The matrix equation, Eq. (35), is solved for a circular cylindrical surface (33). Figure 6 shows the surface current distribution using linear splines and wavelets for different-size cylinders. The wavelet MoM results are compared with the conventional MoM results. To obtain the conventional MoM results, we have used triangular functions for both expanding the unknown current distribution and testing the resultant equation. The conventional MoM results have been verified with a series solution (40). The results of the conventional MoM and the wavelet MoM agree very well.

Next we want to show how "thresholding" affects the final solution. By "thresholding," we mean setting those elements of the matrix to zero that are smaller (in magnitude) than some positive number δ ($0 \leq \delta < 1$), called the threshold parameter, times the largest element of the matrix.

Let $z_{\max}$ and $z_{\min}$ be the largest and the smallest elements of the matrix in Eq. (35). For a fixed value of the threshold parameter δ, define % relative error (ϵ_δ) as (33)

$$\epsilon_\delta := \frac{\|f_0 - f_\delta\|_2}{\|f_0\|_2} \times 100 \tag{39}$$

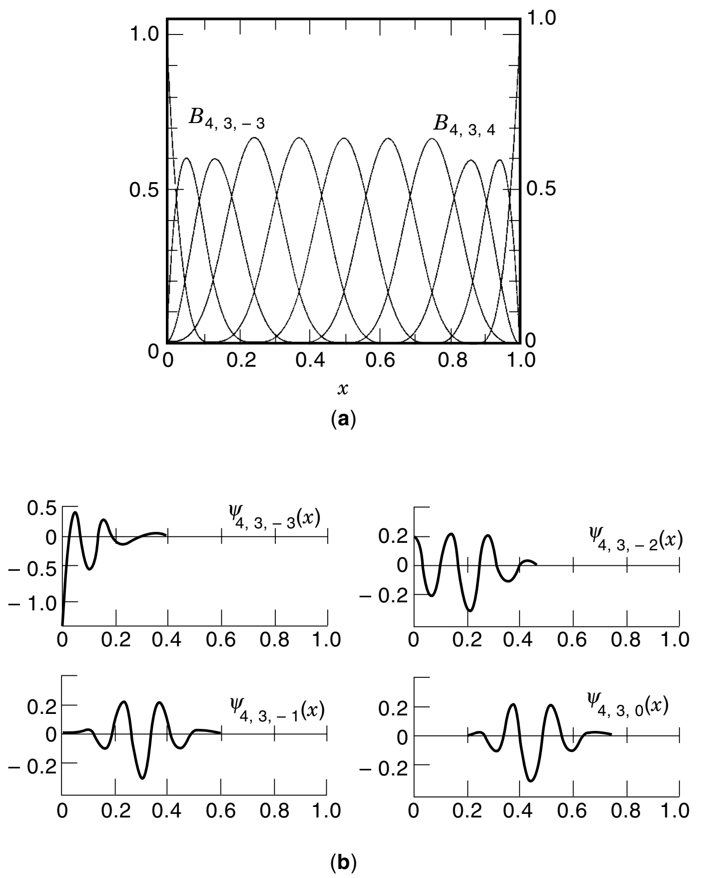

Figure 5. (a) Cubic spline ($m = 4$) scaling functions on [0, 1]. (b) Cubic spline wavelets on [0, 1]. The subscripts indicate the order of spline (m), scale (j), and position (k), respectively (33).

and % sparsity (S_δ) as

$$S_\delta := \frac{N_0 - N_\delta}{N_0} \times 100 \tag{40}$$

In the above, f_δ represents the solution obtained from Eq. (35) when the elements whose magnitudes are smaller than $\delta z_{\max}$ have been set to zero. Similarly, N_δ is the total number of elements left after thresholding. Clearly, $f_0(x) = f(x)$ and $N_0 = N^2$, where N is the number of unknowns.

Table 1 gives an idea of the relative magnitudes of the largest and the smallest elements in the matrix for conventional and wavelet MoM. As is expected, because of their higher vanishing moment property, cubic spline wavelets give the higher ratio, $z_{\max}/z_{\min}$.

Figure 7 shows a typical matrix obtained by applying the conventional MoM. A darker color on an element indicates a larger magnitude. The matrix elements with $\delta = 0.0002$ for the linear spline case are shown in Fig. 8. In Fig. 9, we present the thresholded matrix ($\delta = 0.0025$) for the cubic spline case. The $[Z_{\psi,\psi}]$ part of the matrix is almost diagonalized. Figure 10 gives an idea of the pointwise error in the solution for linear and cubic spline cases.

It is worth pointing out here that regardless of the size of the matrix, only 5×5 in the case of the linear spline and 11×11 in the case of the cubic splines (see the top-left corners of Figs. 8 and 9) will remain unaffected by thresholding;

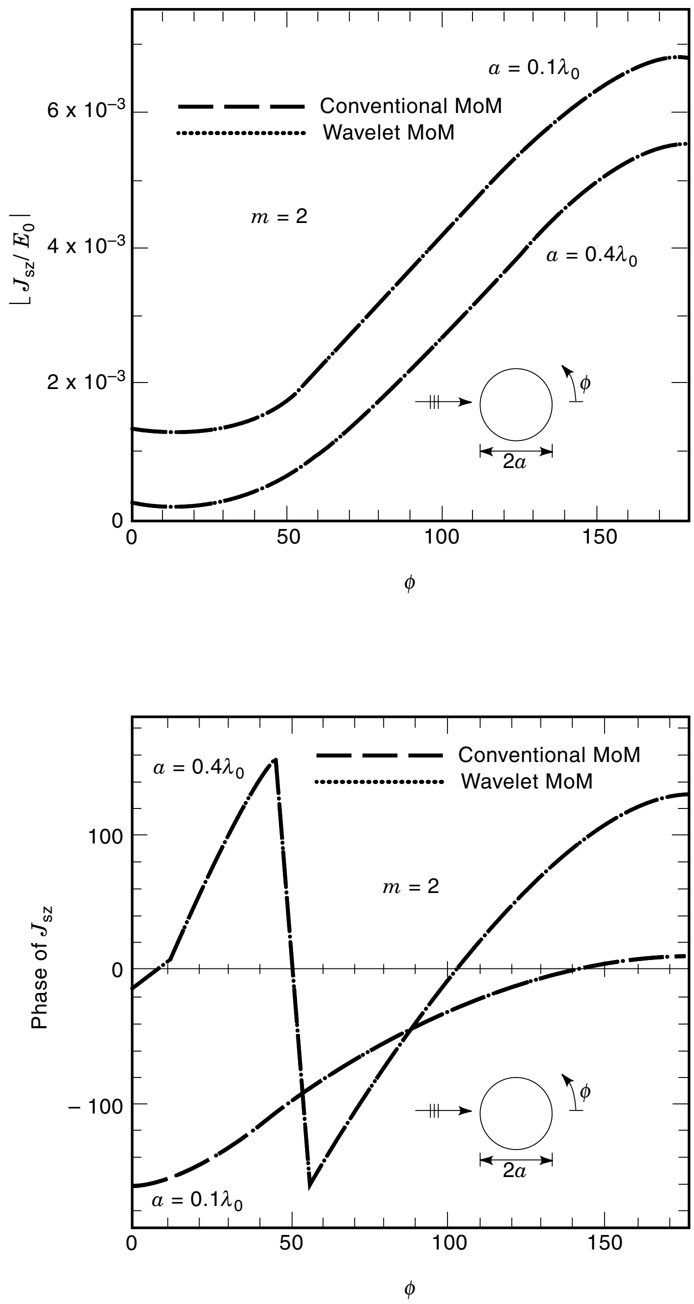

Figure 6. Magnitude and phase of the surface current distribution on a metallic cylinder using linear spline wavelet MoM and conventional MoM. Notice that the results for conventional and wavelet bases completely overlap each other (33).

Table 1. Relative Magnitudes of the Largest and the Smallest Elements of the Matrix for Conventional and Wavelet (33)

	Conventional MoM	Wavelet MoM ($m = 2$)	Wavelet MoM ($m = 4$)
$z_{\max}$	5.377	0.750	0.216
$z_{\min}$	1.682	7.684×10^{-8}	8.585×10^{-13}
Ratio	3.400	9.761×10^{6}	2.516×10^{11}

MoM. $a = 0.1\lambda_0$.

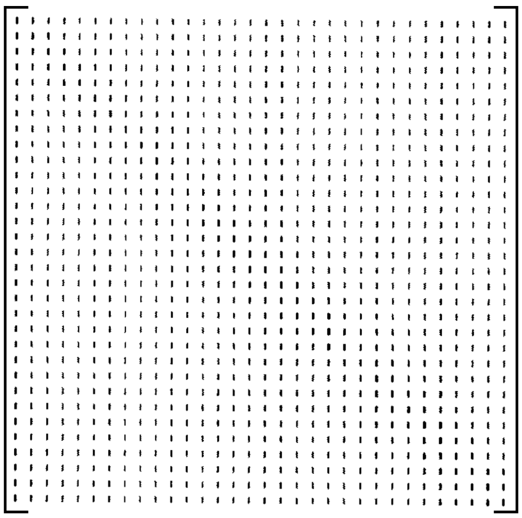

Figure 7. A typical gray-scale plot of the matrix elements obtained using conventional MoM. The darker color represents larger magnitude.

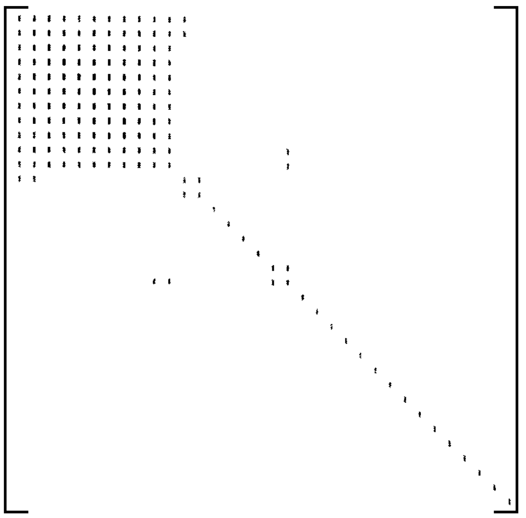

Figure 9. A typical gray-scale plot of the matrix elements obtained using cubic wavelet MoM. The darker color represents larger magnitude.

a significant number of the remaining elements can be set to zero without causing much error in the solution.

SEMIORTHOGONAL VERSUS ORTHOGONAL WAVELETS

Both semiorthogonal and orthogonal wavelets have been used for solving integral equations. A comparative study of their advantages and disadvantages has been reported in Ref. 24. The orthonormal wavelet transformation, because of its unitary similar property, preserves the condition number (κ) of the original impedance matrix Z; semiorthogonal wavelets do not. Consequently, the transformed matrix equation may require more iterations to converge to the desired solution. Some preliminary results comparing the condition number of matrices for different cases are given in Table 2.

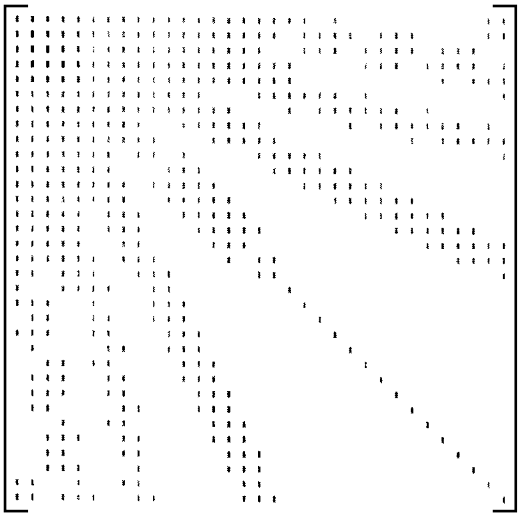

Figure 8. A typical gray-scale plot of the matrix elements obtained using linear wavelet MoM. The darker color represents larger magnitude.

In applying wavelets directly to solve integral equations, one of the most attractive features of semiorthogonal wavelets is that closed-form expressions are available for such wavelets (10,33). Most of the continuous o.n. wavelets cannot be written in closed form. One thing to be kept in mind is that, unlike signal processing applications where one usually deals with a discretized signal and decomposition and reconstruction sequences, here in the boundary value problem we often have to compute the wavelet and scaling function values at any given point. For a strip and thin wire case, a comparison of the computation time and sparsity is summarized in Tables 3 and 4 (24).

Semiorthogonal wavelets are symmetric and hence have a generalized linear phase (5, pp. 160–174), an important factor in function reconstruction. It is well known (4 Sec. 8.1) that symmetric or antisymmetric, real-valued, continuous, and compactly supported o.n. scaling functions and wavelets do not exist. Finally, in using wavelets to solve spectral domain problems, as discussed before, we need to look at the time–frequency window product of the basis. Semiorthogonal wavelets approach the optimal value of the time-frequency product, which is 0.5, very fast. For instance, this value for the cubic spline wavelet is 0.505. It has been shown (41) that this product approaches to ∞ with the increase in smoothness of o.n. wavelets.

DIFFERENTIAL EQUATIONS

An ordinary differential equation (ODE) can be represented as

$$Lf(x) = g(x); x \in [0, 1] \tag{41}$$

with

$$L = \sum_{j=0}^{m} a_j(x) \frac{d^j}{dx^j} \tag{42}$$

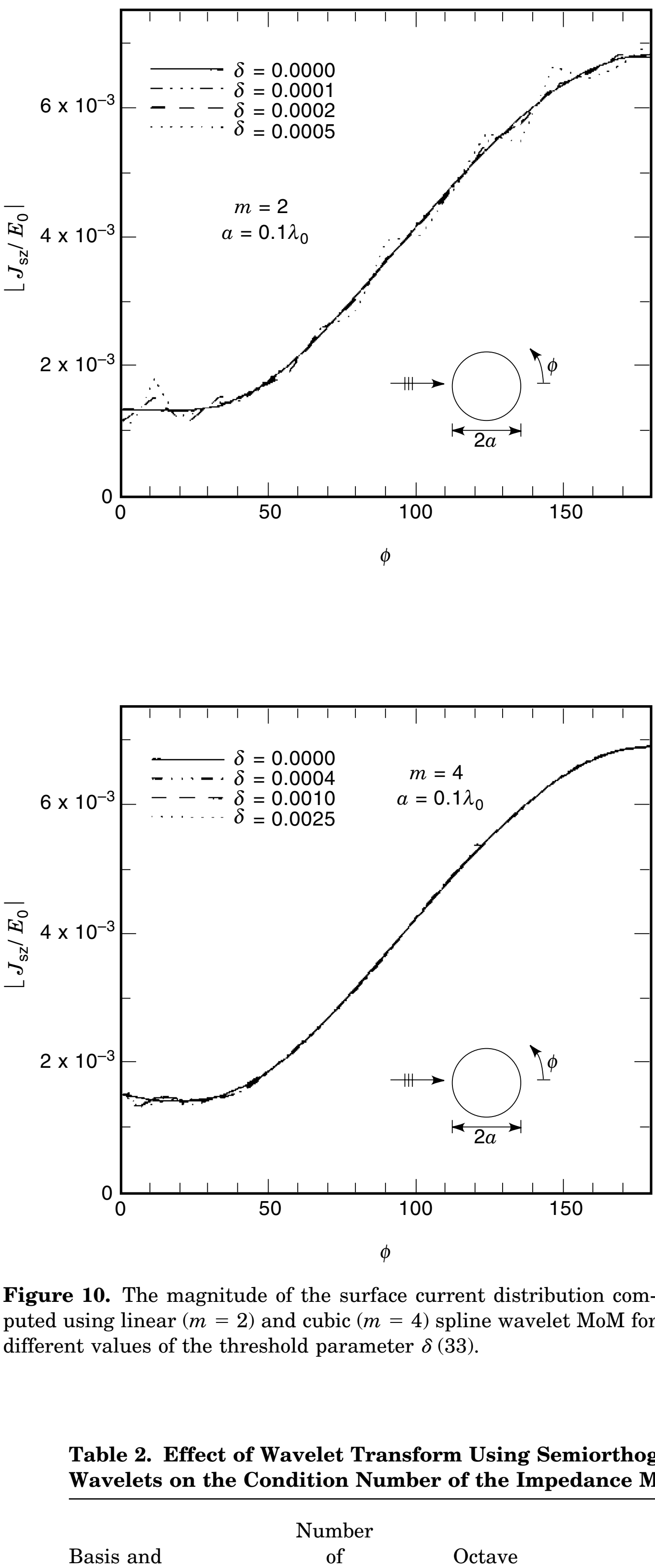

Figure 10. The magnitude of the surface current distribution computed using linear ($m = 2$) and cubic ($m = 4$) spline wavelet MoM for different values of the threshold parameter δ (33).

Table 3. Comparison of CPU Time per Matrix Element for Spline, Semiorthogonal, and Orthonormal Basis Function (24)

	Wire	Plate
Spline	0.12 s	0.25×10^{-3} s
s.o. Wavelet	0.49 s	0.19 s
o.n. Wavelet	4.79 s	4.19 s

and some appropriate boundary conditions. If the coefficients $\{a_j\}$ are independent of x, then the solution can be obtained via a Fourier method. However, in the ODE case, with nonconstant coefficients, and in PDEs, we generally use finite-element- or finite-difference-type methods.

In the traditional finite-element method (FEM), local bases are used to represent the unknown function and the solution is obtained by Galerkin's method, similar to the approach described in previous Sections. For the differential operator, we get sparse and banded stiffness matrices that are generally solved using iterative techniques, the Jacobi method for instance.

One of the disadvantages of conventional FEM is that the condition number (κ) of the stiffness matrix grows as $O(h^{-2})$, where h is the discretization step. As a result, the convergence of the iterative technique becomes slow and the solution becomes sensitive to small perturbations in the matrix elements. If we study how the error decreases with iteration in iterative techniques, such as the Jacobi method, we find that the error decreases rapidly for the first few iterations. After that, the rate at which the error decreases slows down (42, pp. 18–21). Such methods are also called "high-frequency methods" since these iterative procedures have a "smoothing" effect on the high-frequency portion of the error. Once the high-frequency portion of the error is eliminated, convergence becomes quite slow. After the first few iterations, if we could re-discretize the domain with coarser grids and thereby go to lower frequency, the convergence rate would be accelerated. This leads us to a multigrid-type method.

Multigrid or hierarchical methods have been proposed to overcome the difficulties associated with the conventional method (42–58). In this technique, one performs a few iterations of the smoothing method (Jacobi-type), and then the intermediate solution and the operator are projected to a coarse grid. The problem is then solved at the coarse grid, and by interpolation one goes back to the finer grids. By going back and forth between finer and coarse grids, the convergence can be accelerated. It has been shown for elliptic PDEs that for wavelet-based multilevel methods, the condition number is

Table 2. Effect of Wavelet Transform Using Semiorthogonal and Orthonormal Wavelets on the Condition Number of the Impedance Matrix[a]

Basis and Transform	Number of Unknowns	Octave Level	δ	S_δ	ϵ_δ	Condition Number κ Before Threshold	Condition Number κ After Threshold
Pulse and none	64	NA	NA	0.0	2.6×10^{-5}	14.7	—
Pulse and s.o.	64	1	7.2×10^{-2}	46.8	0.70	16.7	16.4
Pulse and o.n.	64	1	7.5×10^{-3}	59.7	0.87	14.7	14.5

[a] Original impedance matrix is generated using pulse basis functions.

Table 4. Comparison of Percentage Sparsity (S_δ) and Percentage Relative Error (ϵ_δ) for Semiorthogonal and Orthonormal Wavelet Impedance Matrices as a Function of Threshold Parameter (δ) (24)

Scatterer/Octave Levels	Number of Unknowns s.o.	Number of Unknowns o.n.	Threshold δ	Sparsity S_δ s.o.	Sparsity S_δ o.n.	Relative Error ϵ_δ s.o.	Relative Error ϵ_δ o.n.
Wire/j = 4	29	33	1×10^{-6}	34.5	24.4	3.4×10^{-3}	4.3×10^{-3}
			5×10^{-6}	48.1	34.3	3.9	1.3×10^{-3}
			1×10^{-5}	51.1	36.5	16.5	5.5×10^{-2}
Plate/j = 2, 3, 4	33	33	1×10^{-4}	51.6	28.1	1×10^{-4}	0.7
			5×10^{-4}	69.7	45.9	4.7	5.2
			1×10^{-3}	82.4	50.9	5.8	10.0

independent of the discretization step, that is, $\kappa = O(1)$ (53). The multigrid method is too involved to be discussed in this article. Readers are encouraged to look at the references provided at the end of this article.

Multiresolution aspects of wavelets have also been applied in evolution equations (57,58). In evolution problems, the space and time discretization are interrelated to gain a stable numerical scheme. The time-step must be determined from the smallest space discretization. This makes the computation quite complex. A space-time adaptive method has been introduced in Ref. 58, where wavelets have been used to adjust the space-time discretization steps locally.

BIBLIOGRAPHY

1. G. B. Arfken and H. J. Weber, *Mathematical Methods for Physicists,* San Diego, CA: Academic Press, 1995.
2. Y. Meyer, *Wavelets: Algorithms and Applications,* Philadelphia, PA: SIAM, 1993.
3. S. Mallat, A theory of multiresolution signal decomposition: The wavelet representation, *IEEE Trans. Pattern Anal. Mach. Intell.,* **11**: 674–693, 1989.
4. I. Daubechies, *Ten Lectures on Wavelets,* CBMS-NSF Ser. Appl. Math., No. 61, Philadelphia, PA: SIAM, 1992.
5. C. K. Chui, *An Introduction to Wavelets,* Boston: Academic Press, 1992.
6. C. K. Chui, *Wavelets: A Mathematical Tool for Signal Analysis,* Philadelphia, PA: SIAM, 1997.
7. G. Strang and T. Nguyen, *Wavelets and Filter Banks,* Wellesley, UK: Wellesley-Cambridge Press, 1996.
8. M. Vetterli and J. Kovačević, *Wavelets and Subband Coding,* Upper Saddle River, NJ: Prentice-Hall, 1995.
9. A. N. Akansu and R. A. Haddad, *Multiresolution Signal Decomposition,* San Diego, CA: Academic Press, 1992.
10. J. C. Goswami and A. K. Chan, *Fundamentals of Wavelets: Theory, Algorithms, and Applications,* New York: Wiley, 1999.
11. A. Cohen, I. Daubechies, and J. C. Feauveau, Biorthonormal bases of compactly supported wavelets, *Commun. Pure Appl. Math.,* **45**: 485–500, 1992.
12. G. M. Wing, *A Primer on Integral Equations of the First Kind,* Philadelphia, PA: SIAM, 1991.
13. J. H. Richmond, Digital solutions of the rigorous equations for scattering problems, *Proc. IEEE,* **53**: 796–804, 1965.
14. B. K. Alpert et al., Wavelet-like bases for the fast solution of second-kind integral equations, *SIAM J. Sci. Comput.,* **14**: 159–184, 1993.
15. J. Mandel, On multi-level iterative methods for integral equations of the second kind and related problems, *Numer. Math.,* **46**: 147–157, 1985.
16. J. C. Goswami, An application of wavelet bases in the spectral domain analysis of transmission line discontinuities, *Int. J. Numer. Model.,* **11**: 41–54, 1998.
17. R. F. Harrington, *Field Computation by Moment Methods,* New York: IEEE Press, 1992.
18. G. Beylkin, R. Coifman, and V. Rokhlin, Fast wavelet transform and numerical algorithms I, *Commun. Pure Appl. Math.,* **44**: 141–183, 1991.
19. R. L. Wagner, P. Otto, and W. C. Chew, Fast waveguide mode computation using wavelet-like basis functions, *IEEE Microw. Guided Wave Lett.,* **3**: 208–210, 1993.
20. H. Kim and H. Ling, On the application of fast wavelet transform to the integral-equation of electromagnetic scattering problems, *Microw. Opt. Technol. Lett.,* **6**: 168–173, 1993.
21. B. Z. Steinberg and Y. Leviatan, On the use of wavelet expansions in method of moments, *IEEE Trans. Antennas Propag.,* **41**: 610–619, 1993.
22. K. Sabetfakhri and L. P. B. Katehi, Analysis of integrated millimeter-wave and submillimeter-wave waveguides using orthonormal wavelet expansions, *IEEE Trans. Microw. Theory Tech.,* **42**: 2412–2422, 1994.
23. B. Z. Steinberg, A multiresolution theory of scattering and diffraction, *Wave Motion,* **19** (3): 213–232, 1994.
24. R. D. Nevels, J. C. Goswami, and H. Tehrani, Semi-orthogonal versus orthogonal wavelet basis sets for solving integral equations, *IEEE Trans. Antennas Propag.,* **45**: 1332–1339, 1997.
25. Z. Xiang and Y. Lu, An effective wavelet matrix transform approach for efficient solutions of electromagnetic integral equations, *IEEE Trans. Antennas Propag.,* **45**: 1205–1213, 1997.
26. Z. Baharav and Y. Leviatan, Impedance matrix compression (IMC) using iteratively selected wavelet basis, *IEEE Trans. Antennas Propag.,* **46**: 226–233, 1997.
27. R. D. Nevels and R. E. Miller, A comparison of moment impedance matrices obtained by direct and transform matrix methods using wavelet basis functions, *IEEE Trans. Antennas Propag. Soc. Int. Symp.,* 1997.
28. B. Z. Steinberg and Y. Leviatan, Periodic wavelet expansions for analysis of scattering from metallic cylinders, *IEEE Antennas Propag. Soc. Symp.,* 1994, pp. 20–23.
29. G. W. Pan and X. Zhu, The application of fast adaptive wavelet expansion method in the computation of parameter matrices of multiple lossy transmission lines, *IEEE Antennas Propag. Soc. Symp.,* 1994, pp. 29–32.
30. G. Wang, G. W. Pan, and B. K. Gilbert, A hybrid wavelet expansion and boundary element analysis for multiconductor transmis-

sion lines in multilayered dielectric media, *IEEE Trans. Microw. Theory Tech.,* **43**: 664–675, 1995.

31. W. L. Golik, Wavelet packets for fast solution of electromagnetic integral equations, *IEEE Trans. Antennas Propag.,* **46**: 618–624, 1998.
32. *Int. J. Numerical Modeling: Electron. Netw., Devices Fields,* Special Issue on Wavelets in Electromagnetics, **11**: 1998.
33. J. C. Goswami, A. K. Chan, and C. K. Chui, On solving first-kind integral equations using wavelets on a bounded interval, *IEEE Trans. Antennas Propag.,* **43**: 614–622, 1995.
34. C. K. Chui, J. C. Goswami, and A. K. Chan, Fast integral wavelet transform on a dense set of time-scale domain, *Numer. Math.,* **70**: 283–302, 1995.
35. J. C. Goswami, A. K. Chan, and C. K. Chui, On a spline-based fast integral wavelet transform algorithm, in H. L. Bertoni et al. (eds.), *Ultra-Wideband Short Pulse Electromagnetics 2,* New York: Plenum, 1995, pp. 455–463.
36. J. C. Goswami, A. K. Chan, and C. K. Chui, An application of fast integral wavelet transform to waveguide mode identification, *IEEE Trans. Microw. Theory Tech.,* **43**: 655–663, 1995.
37. E. Quak and N. Weyrich, Decomposition and reconstruction algorithms for spline wavelets on a bounded interval, *Appl. Comput. Harmonic Anal.,* **1**: 217–231, 1994.
38. A. Cohen, I. Daubechies, and P. Vial, Wavelets on the interval and fast wavelet transform, *Appl. Comput. Harmonic Anal.,* **1**: 54–81, 1993.
39. P. Auscher, Wavelets with boundary conditions on the interval, in C. K. Chui (ed.), *Wavelets: A Tutorial in Theory and Applications,* Boston: Academic Press, 1992, pp. 217–236.
40. R. F. Harrington, *Time-Harmonic Electromagnetic Fields,* New York: McGraw-Hill, 1961.
41. C. K. Chui and J. Z. Wang, High-order orthonormal scaling functions and wavelets give poor time-frequency localization, *Fourier Anal. Appl.,* **2**: 415–426, 1996.
42. W. Hackbusch, *Multigrid Methods and Applications,* New York: Springer-Verlag, 1985.
43. A. Brandt, Multi-level adaptive solutions to boundary value problems, *Math. Comput.,* **31**: 330–390, 1977.
44. W. L. Briggs, *A Multigrid Tutorial,* Philadelphia, PA: SIAM, 1987.
45. S. Dahlke and I. Weinreich, Wavelet–Galerkin methods: An adapted biorthogonal wavelet basis, *Construct. Approx.,* **9**: 237–262, 1993.
46. W. Dahmen, A. J. Kurdila, and P. Oswald (eds.), *Multiscale Wavelet Methods for Partial Differential Equations,* San Diego, CA: Academic Press, 1997.
47. H. Yserentant, On the multi-level splitting of finite element spaces, *Numer. Math.,* **49**: 379–412, 1986.
48. J. Liandrat and P. Tchamitchian, Resolution of the 1-D regularized Burgers equation using a spatial wavelet approximation, *NASA Rep. ICASE,* **90-83**: 1990.
49. R. Glowinski et al., Wavelet solution of linear and nonlinear elliptic, parabolic, and hyperbolic problems in one space dimension, in R. Glowinski and A. Lichnewsky (eds.), *Computing Methods in Applied Sciences and Engineering,* Philadelphia. PA: SIAM, 1990, pp. 55–120.
50. P. Oswald, On a hierarchical basis multilevel method with nonconforming P1 elements, *Numer. Math.,* **62**: 189–212, 1992.
51. W. Dahmen and A. Kunoth, Multilevel preconditioning, *Numer. Math.,* **63**: 315–344, 1992.
52. P. W. Hemker and H. Schippers, Multiple grid methods for the solution of Fredholm integral equations of the second kind, *Math. Comput.,* **36** (153): 215–232, 1981.
53. S. Jaffard, Wavelet methods for fast resolution of elliptic problems, *SIAM J. Numer. Anal.,* **29**: 965–986, 1992.
54. S. Jaffard and P. Laurençot, Orthonomal wavelets, analysis of operators, and applications to numerical analysis, in C. K. Chui (ed.), *Wavelets: A Tutorial in Theory and Applications,* Boston: Academic Press, 1992, pp. 543–601.
55. J. Xu and W. Shann, Galerkin–wavelet methods for two-point boundary value problems, *Numer. Math.,* **63**: 123–144, 1992.
56. C. Guerrini and M. Piraccini, Parallel Wavelet–Galerkin methods using adapted wavelet packet bases, in C. K. Chui and L. L. Schumaker (eds.), *Wavelets and Multilevel Approximation,* River Edge, NJ: World Scientific, 1995, pp. 133–142.
57. M. Krumpholz and L. P. B. Katehi, MRTD: New time-domain schemes based on multiresolution analysis, *IEEE Trans. Microw. Theory Tech.,* **44**: 555–571, 1996.
58. E. Bacry, S. Mallat, and G. Papanicolaou, A wavelet based space-time adaptive numerical method for partial differential equations, *Math. Model. Numer. Anal.,* **26**: 793–834, 1992.

JAIDEVA C. GOSWAMI
Sugar Land Product Center
RICHARD E. MILLER
ROBERT D. NEVELS
Texas A&M University